Instability of Flow with Temperature-Dependent Viscosity: A Model of Magma Dynamics

J. A. WHITEHEAD AND KARL R. HELFRICH

Woods Hole Oceanographic Institution, Woods Hole, Massachusetts

In material whose viscosity is very temperature dependent, flow from a chamber through a cooled slot can develop a fingering instability or time-dependent behavior, depending on the elastic properties of the chamber, the viscosity-temperature relationship, and the geometry of the slot. A laboratory experiment is described where syrup flows from a reservoir through a tube immersed in a chilled bath to an exit hole at constant pressure. Flow is either steady or periodic depending on the temperature of the bath and the flow rate into the reservoir. A theory indicates that the transition from steady to periodic flow depends on nonlinearities in the steady state relation between pressure and flow rate. A general stability criterion is advanced that states that the Peclet number must be within a certain range for instability to develop. Parameters governing the oscillation period are determined. Theory also indicates that flow through a slot would develop finger-like instabilities under certain conditions. Qualitative laboratory experiments with paraffin spreading over a cold plate reveal the fingering.

1. INTRODUCTION

There are many examples in geophysics where hot material from deep in the Earth flows to the surface, where it then cools, slows down and may ultimately even stop from that cooling. Obvious examples are found in volcanic magma flows, where stoppage is ultimately produced by solidification of the material. However, before the complete solidification is consummated, flow resistance can increase from the action of numerous processes that retard the flow upon cooling of the magma. Some examples of processes that increase the resistance of magmas flows are [Hughes, 1982] constriction of the pipes and conduits from deposition of crystals along the wall; an increase in fluid viscosity due to cooling; an increase in viscosity due to bulk composition changes through preferential crystallization; and the addition of suspended crystals to the fluid upon cooling, with a consequent dramatic increase in bulk viscosity. One wonders whether novel flow structures such as fingers, time-dependent surges, and complicated free surface shapes such as pahoehoe or pillow lavas are the result of this increase in resistance.

Magmatic systems are not the only flowing systems that encounter an increase of resistance upon cooling. Many aquifers dissolve away minerals under high pressure and temperature and some of these minerals may be redeposited along the walls in other locations of the system where there are lower pressures or temperatures. There are numerous cases both in terrestrial and deep-sea hydrothermal springs where the systems pulsate, become restricted to a few localized springs, or ultimately become clogged by the deposited minerals.

The purpose of this study is to investigate the dynamics of flows that develop increased resistance as they flow into cooler regions and particularly to understand a dynamic instability that develops. The instability is characterized by the development of fingers of melt-and time-dependent flows. We believe that this is one of the most prevalent processes in the cooling of hot geological and geophysical systems. The approach is to study simple problems, to illustrate the features that develop, and to suggest possible applications. Duplication of full geological complexity is beyond our capabilities and in any case could only be done on a case by case basis.

The closest analogy known to this situation is Saffman-Taylor instability [Saffman and Taylor, 1958], in which a fluid intrudes into a porous region or a Hele-Shaw cell (two plane walls separated by a small gap) that contains a second more viscous fluid. Under suitable conditions, the interface between the two fluids will develop finger-like protrusions that contain the lower-viscosity fluid and extend into the viscous fluid. The lower-viscosity fluid possesses less hydraulic resistance to the large-scale pressure field and moves rapidly into the finger. This forces the finger tip to advance farther into the viscous fluid. The examples of Saffman-Taylor instability that have been studied to date, whether with mathematical analysis or with laboratory experiments, are inherently time dependent, and the tips continue to move indefinitely. After a long time the region is filled with veins of the low-viscosity fluid; each vein is surrounded by islands of viscous fluid that are slowly moving away from the source. The final state is never truly steady.

An analysis similar to that of Saffman-Taylor but with more direct geochemical applications was conducted by Ortoleva, et al., [1987a]. In their problem, an advancing front reacted with host material to produce scallops. They suggest that numerous geological features may be generated by this geochemical self-organization Ortoleva, et al., [1987b]. A second physical process for thermal control of basaltic eruptions has been recently developed by Bruce and Huppert [1989]. Melt flowing through a dyke is shown to be fundamentally unsteady and either gradually blocks or melts back the walls of the dyke. It was pointed out that these results show that such a process leads to flow localization as hypothesized by McBirney [1984].

Here, a thermal approach similar to that of Bruce and Huppert is combined with instability considerations to pro-

duce a thermal equivalent to either the Saffman-Taylor instability or the geochemical self-organization. Instead of two materially differing fluids we will have one fluid with temperature-dependent viscosity. It will flow from the source as a hot fluid and will be cooled through thermal conduction to the cold sidewalls of a Hele-Shaw cell. Unlike the previously studied problems, the final state may become truly steady (although periodic or chaotic states are also possibilities). The only similiar study is by S. Morris (private communication, 1989), who predicts instability in the above problem in a semi-infinite half-space.

In section 2 we describe a laboratory experiment that illustrates one possible situation, when hot fluid flows through a cold pipe from an elastic reservoir. The flow is found to be either steady or periodic, depending on the amount of increase in viscosity that is produced in the cold region and the replenishment rate of the reservior.

In section 3 a simple theory is advanced to explain the observed behavior. A stability analysis is conducted for an idealized problem with flow from an elastic chamber through a slot. In the one-dimensional limit corresponding to the experiments in section 2, the theory predicts linear instability for certain parameter ranges. The nonlinear theory shows that a limit cycle oscillation will result. For two-dimensional flow, linear theory predicts a spatial fingering instability which would laterally concentrate the flow in the slot.

In section 4 a second type of laboratory experiment is described with paraffin spreading radially from a point source over a cold plate. It is found that when the Peclet number is of order 1, the radially symmetric flow experiences a transition to a fingering flow. At first, a number of fingers are visible at the outer front of the expanding circular pool of paraffin. In the intermediate stage, these fingers advance substantially. Each finger is fed by a tube of flowing melted paraffin. The rest of the paraffin stops and ultimately solidifies. At a later time all but one of the tubes slow down and stop, and the melted paraffin flows only in one tube for as long as the experiment continues. The paraffin everywhere else gradually solidifies.

Both the laboratory experiments and the theory indicate that the flow rate must lie within a certain range for instability so that a suitably defined Peclet number is of order one. Both flow below this range, and flow above this range will produce decaying infinitesimal perturbations. Linearly unstable flow can develop oscillatory instabilities or spatially periodic instabilities.

2. A LABORATORY EXPERIMENT WITH COOLED CORN SYRUP

The apparatus (Figure 1) consisted of a vertical glass tube 3.8 cm inside diameter and 1 m long located below a reservoir containing "Karo" brand corn syrup. A variable control valve leading from the reservoir allowed syrup to fall into the glass tube at a controlled rate. Projecting out of the bottom of the glass tube was a stopper with a hole and a 0.383 cm inside diameter copper tube. Various lengths were used. The copper tube projected downward and was shaped like the letter "j". The lowest part to the "j" was immersed in a refrigerated thermostatic bath, and a flexible plastic tube extended from the end of the copper tube to a point outside the bath over a beaker placed to catch outflow. In an
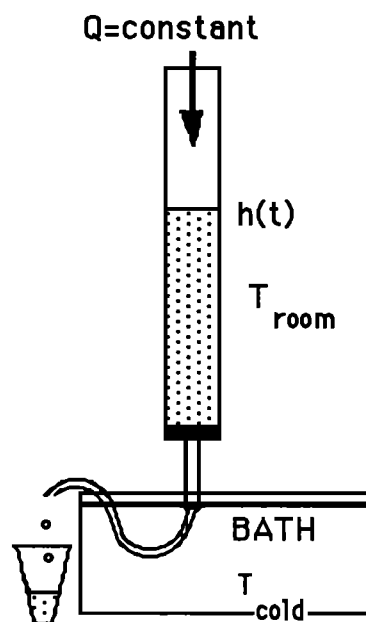

Fig. 1. Sketch of the apparatus for generating flow modulation from temperature-dependent viscosity. Corn syrup is fed into a horizontal tube at a constant rate. As the syrup accumulates, it increases pressure across a small outlet tube that is in contact with a cold bath. When the syrup flows rapidly, it stays hot, but when it flows slowly, it gets very cold and viscous.

experiment, syrup flowed from the reservoir into the tube. Syrup in the glass tube builds up to a height h that can be easily measured and flows out through the bottom copper tube. The frictional resistance to flow takes place principally in the copper tube because it is much smaller that the glass tube. As the syrup flows out, it is cooled by thermal conduction through the copper tube.

The apparatus was intended to be a simple upside down model of a magma system. The glass tube represents a compressible magma chamber, the height of the free surface in the glass tube represents pressure in the chamber, and the copper tube in the refrigerated bath represents magma flowing to the surface of the Earth through cracks or fissures. It was hoped that if the refrigerator was sufficiently cold and if the syrup has a sufficiently great viscosity upon cooling, that an unsteady flow would develop even if flow from the reservoir was steady. Some estimate of how much viscosity change was necessary was obtained from the theoretical considerations in section 3.

First, simple run-down experiments were conducted to obtain some estimate of the resistance as a function of the flow rate. Theoretical considerations in section 3 indicated that time dependence was not to be expected unless resistance could be made to be inversely proportional to flow rate. Figure 2 shows data from two runs. The first (left) had a bath temperature set to 0°C, a room temperature of 24.1°C and with a copper tube 30 cm long; the second (right) had a bath temperature of −11.0°C, a room temperature of 24.0°C, and a copper tube 14.5 cm. long. Figures 2a and 2b show height versus time, from which the height versus velocity were determined to give Figures 2c and 2d. For the 0°C run, the run-down is close to exponential (which one would expect for a strictly uniform viscosity). In contrast,
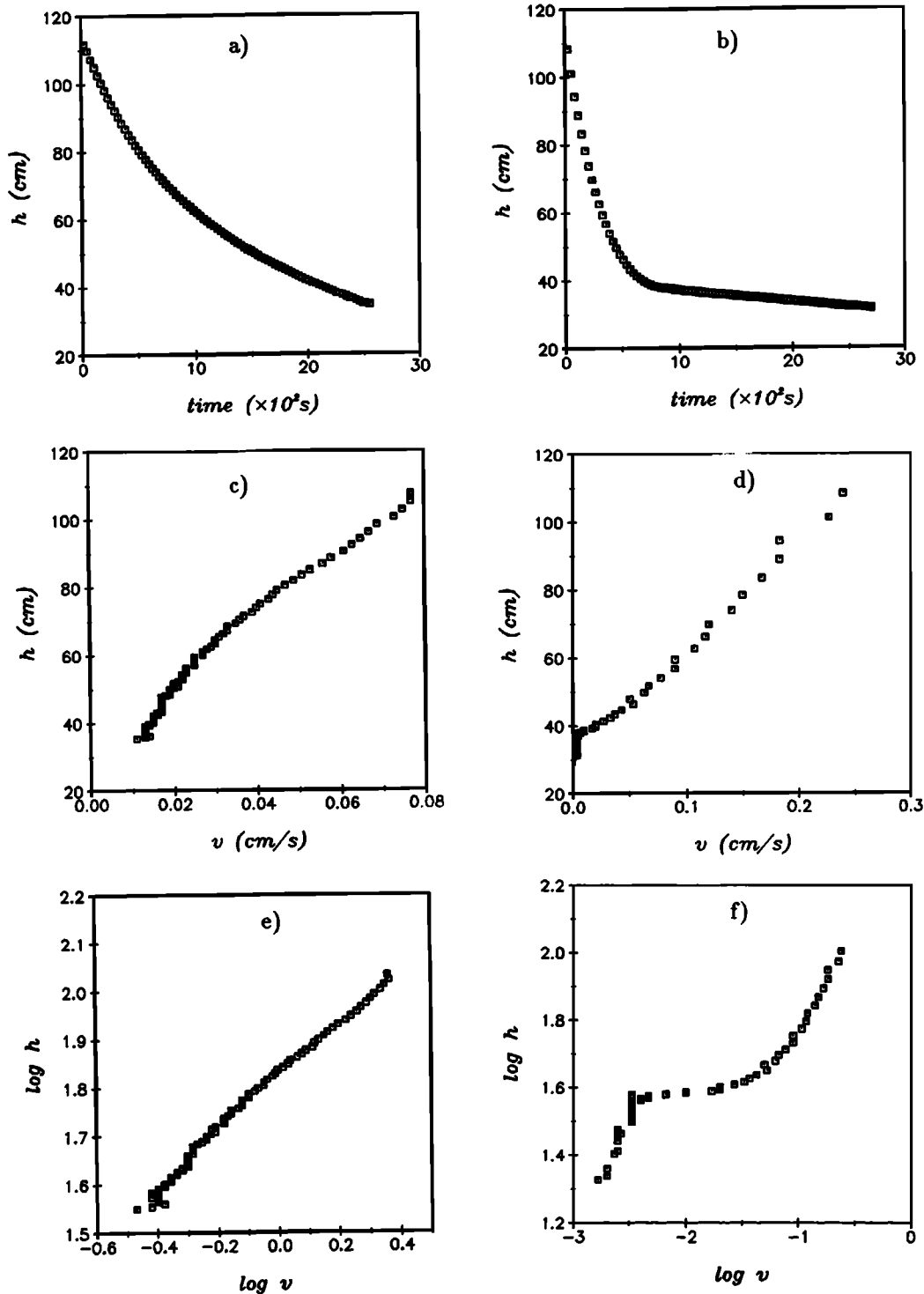
Fig. 2. Results from two run down experiments with different bath temperatures. On the left, (Figures 2a, 2c and 2e) the bath is at 0°C, and on the right (Figure 2b, 2d, and 2f) the bath is at −11.0°C. Height versus time is plotted in (Figures 2a, 2b), height versus velocity is plotted in Figures 2c, 2d), and log height versus log velocity is plotted for (Figures 2e, 2f).

the −11.0°C run was similar to the first run for only roughly the first thousand seconds, then there was a transition to a very much slower run-down. Presumably at the later time the viscosity of the syrup is very large due to cooling in the copper tube. The difference between the two states is particularly clear on the height versus velocity plot (Figures 2c, and 2d) and even more so when shown as a log-log plot

(Figures 2e, and 2f). For the run at −11.0°C, the transition region from fast to slow run-down is characterized by a plateau in the height-velocity logarithmic curve. Considerations developed in the theoretical section will illustrate the significance of the plateau.

When the volume flux of the source was set at a value corresponding to the middle of the plateau, the height oscil-

lated with time. Figure 3 shows height versus time, height versus velocity and the log height versus log velocity for one example. This run was started as a run-down, but then the volume flux from the reservoir was turned on at the time denoted by the arrow shown in Figure 3a. Three complete and nearly identical oscillations were seen thereafter. The plot
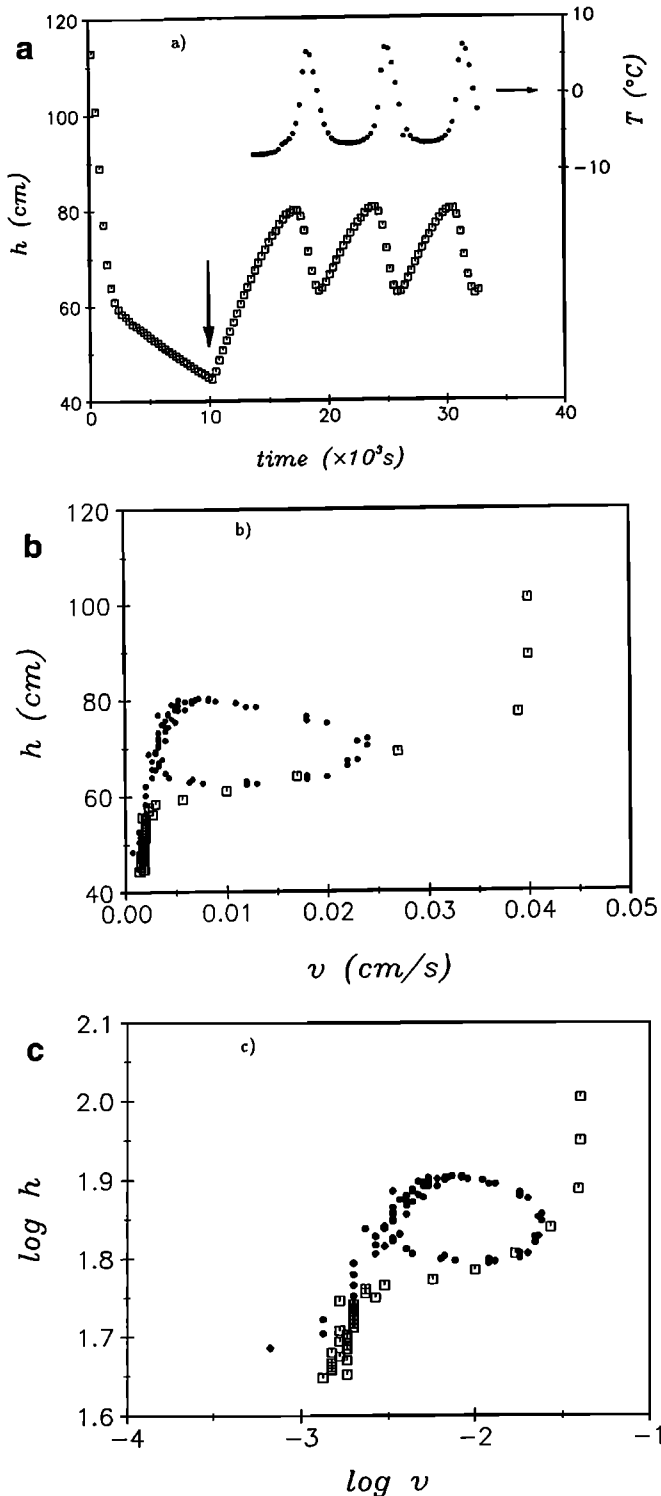

Fig. 3. An experiment that first had a run-down and then had a steady source turned on at the time shown by the arrow in 3a. Plotted are (a) height and temperature versus time, (b) height versus velocity, and (c) log height versus log velocity.

of height versus velocity was made from these data, but it was necessary to subtract the constant velocity of the source from the time derivative of the height record to determine velocity out of the end of the tube. This was accomplished by measuring the abrupt change in slope immediately before and after the arrow. The oscillations produce a closed curve in height-velocity space that lies on the top of the plateau from the run-down portion of the experiment. The plots of the logarithms (Figure 3c) more clearly show the limit cycle oscillation on the plateau.

Additional runs have verified the reproducibility of the oscillations when the parameters were set close to those in Figure 3. When the flow rate of the source was set at a value outside the plateau or when the bath was set at 0°C, no oscillations were found, and the height would asymptotically approach a steady value.

The experiments exhibited a transition from steady flow to a more complicated flow when the velocity w ranged between 0.003 and 0.03 cm/s. Peclet numbers wr/κ (see section 3) based upon the above velocities, a radius r of 0.2 cm, and thermal diffusivity $\kappa = 1 \times 10^{-3}$ cm^2/s, range from 0.6 to 6. The parameter $wr^2/\kappa L$, where L is the length of the copper tube, ranged from 0.01 to 0.1.

3. STABILITY OF UNIFORM FLOW

The purpose of this section is to develop a theory for hot fluid flowing through a slot that is cooled from the sidewalls. A slot, rather than a circular tube, is incorporated so that spatial, as well as time-dependent, instabilities may be investigated. It will be shown that both temporal and spatial instabilities are expected for Peclet numbers within a certain range.

Consider the simple system sketched in Figure 4. A narrow slot with cooled walls is fed from below by fluid in a hot chamber. The bottom of the chamber is fed by a uniform volumetric flux per unit length Q. The slot width is d and the slot height is L. Take the chamber to be elastic so that pressure in the chamber is related to inflation or deflation of the chamber by the formula

$$E^{-1} \frac{\partial p}{\partial t} = Q - wd - \overline{A} \frac{\partial v}{\partial y} \qquad (1)$$

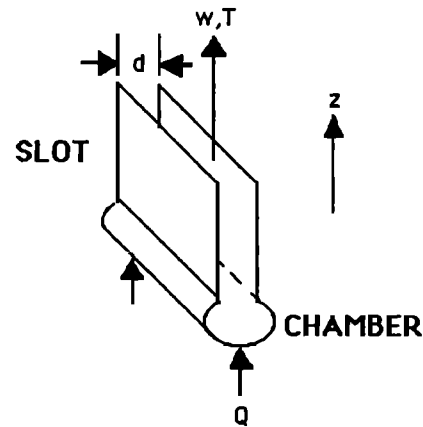where $\overline{A}$ is cross-sectional area of the chamber, which we

Fig. 4. Sketch of the idealized system. A constant flux Q comes in at the bottom of the chamber. It can flow up the slot with local velocity w and cool through the side walls. It can also flow along the chamber. The chamber has elastic walls.

have taken as a constant on the right-hand side in order to keep (1) linear. Here E is a positive coefficient of elasticity, and velocity v is the velocity along the chamber axis. E^{-1} is analogous to glass tube area and p is analogous to H in the experiment in section 2. In the chamber, we assume there is Poiseuille flow, so there is a balance between viscous resistance from velocity v and along-chamber pressure drop, so that

$$\frac{\nu_H v}{\ell_c^2} = -\frac{1}{\rho}\frac{\partial p}{\partial y} \qquad (2)$$

where ν_H is the viscosity of the hot fluid in the chamber and ℓ_c^2 is a length scale of the chamber. Combining (1) and (2),

$$E^{-1}\frac{\partial p}{\partial t} = Q - wd + \frac{\overline{A}\ell_c^2}{\nu_H\rho}\frac{\partial^2 p}{\partial y^2} \qquad (3)$$

If we assume that the vertical flow in the slot is independent of the across-slot direction, the viscous flow is governed by

$$\frac{\partial w}{\partial t} + \frac{12\nu(T)}{d^2}\,w = -\frac{1}{\rho}\frac{\partial p}{\partial z} \qquad (4)$$

where the viscosity

$$\nu = \nu_H + \alpha(T_H - T) \qquad (5)$$

and T is the temperature of the fluid in the slot.

It is desired to find the pressure drop through the slot (i.e., resistance to the flow) as a function of w. To do this, it is necessary to determined the temperature in the slot, which can be found analytically under certain assumptions. First, we look at steady flow through the slot and assume that the material is flowing as a uniform slab so that

$$w\frac{\partial T}{\partial z} = \kappa\frac{\partial^2 T}{\partial x^2} \qquad (6)$$

Let the temperature of the boundary decrease linearly in the z direction at a rate $\Delta T/L$ so

$$T = T_H - \frac{\Delta T}{L}\,z \qquad \text{at} \qquad |\,x\,| = d/2 \qquad (7)$$

A particular solution to (6) and (7) of the form

$$T = T_H - \frac{\Delta T}{L}\,z + \frac{w\Delta T}{2\kappa L}\left(\frac{d^2}{4} - x^2\right) \qquad (8)$$

exists. A homogeneous solution $\tilde{T}\,(x, z)$ must be added to (8) to match the boundary condition $T = T_H$ at $z = 0$. The homogeneous solution gives the boundary layer adjustment at the entrance, and decays rapidly to zero with an e-folding scale $\sim wd^2/\kappa\pi^2$. Rather than use the combersome full solution, we will approximate the centerline ($x = 0$), temperature by T_H for $z < wd^2/8\kappa$ and by (8) with $x = 0$ for $wd^2/8\kappa < z < L$. The temperature of the sidewall and the centerline is sketched in Figure 5 .

It is helpful to inspect a solution to the momentum equation (4) with $\partial w/\partial t = 0$ and ν given by (5). The temperature along the centerline is used to give

$$\frac{p_0}{\rho} = \frac{12w}{d^2}\left\{\int_0^L \nu_H dz +\right.$$

$$\left.\int_{\frac{wd^2}{8\kappa}}^L \alpha\left(\frac{\Delta Tz}{L} - \frac{wd^2\Delta T}{8\kappa L}\right)dz\right\} \qquad (9)$$
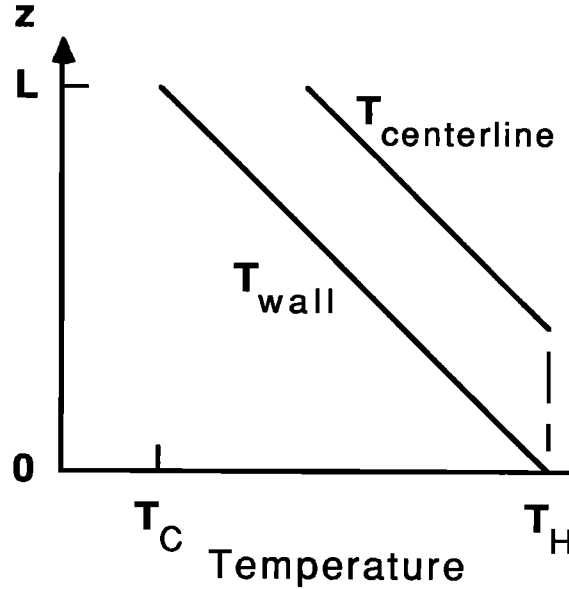
Thus

$$\frac{p_0}{\rho} =$$

Fig. 5. Sketch of the temperature of the wall and the temperature of the centerline of the fluid for this idealized problem.

$$\begin{cases} \frac{12w}{d^2} & \left(\nu_H L + \frac{\alpha\Delta T}{2L}\left(L - \frac{wd^2}{8\kappa}\right)^2\right) & w \le \frac{8\kappa L}{d^2} \\ \frac{12\nu_H Lw}{d^2} & & w > \frac{8\kappa L}{d^2} \end{cases} \qquad (10)$$

which can be normalized to

$$p_0' =$$

$$\frac{p_0 d^2}{\rho 12\nu_H Lw_r} = \begin{cases} \frac{w}{w_r}\left(1 + \frac{A}{2}\left(1 - \frac{w}{w_r}\right)^2\right) & w \le w_r \\ \frac{w}{w_r} & w > w_r \end{cases} \qquad (11)$$

Here

$$w_r = \frac{8\kappa L}{d^2} \qquad (12)$$

and

$$A = \frac{\alpha\Delta T}{\nu_H} \qquad (13)$$

Figure 6 is a plot of equation (11) for three values of A. An important physical result is that for $A > 6$ pressure can drop off with an increase in velocity over the range

$$\frac{2}{3}\left[1 - \frac{1}{2}(1 - \frac{6}{A})^{\frac{1}{2}}\right] < \frac{w}{w_r} < 1 \qquad (14)$$

The lower limit of the inequality is equal to $2/3$ when $A = 6$, and is equal to $1/3$ for $A \gg 6$. In dimensional terms this gives a pressure drop off with an increase in velocity for

$$\frac{2}{3} < \frac{wd^2}{8\kappa L} < 1 \qquad \text{for } A = 6$$

and

$$\frac{1}{3} < \frac{wd^2}{8\kappa L} < 1 \qquad \text{for } A \gg 6$$

This parameter range is extremely important because a drop off in pressure with an increase in velocity leads to various instabilities to the uniform flow as observed in the experiment. The stability equations will now be derived.
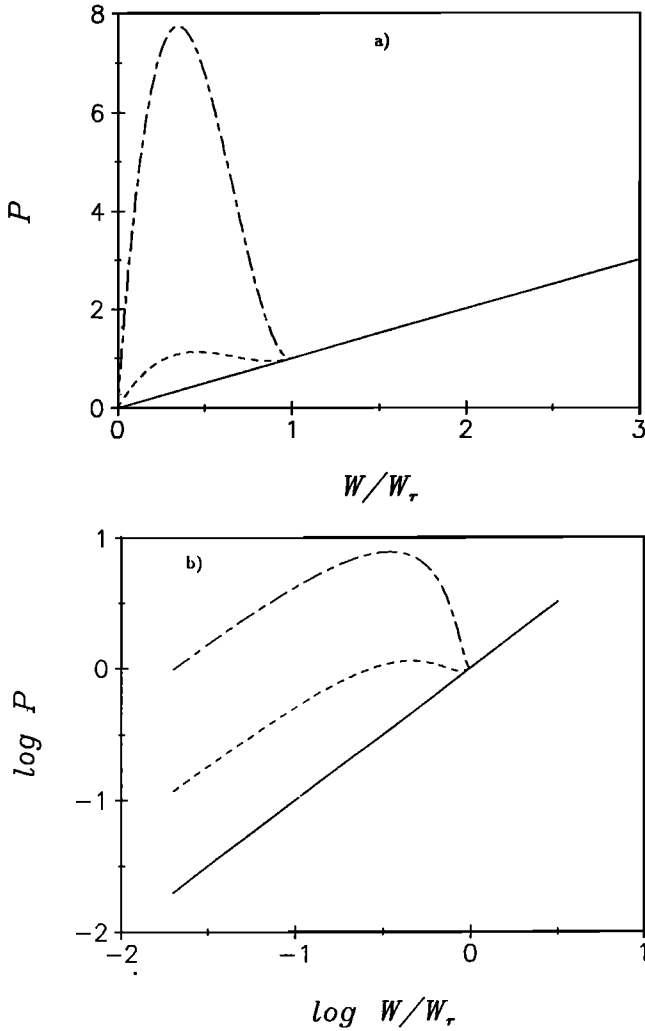
Fig. 6. (a) Pressure drop across the slot calculated from equation (11) as a function of velocity of the fluid for the three values $A = 0$ (solid curve), 10 (dashed curve), and 100 (dash-dot curve). (b) The same data plotted as log-log.

Assuming that the viscous resistance in the slot can be approximated by the steady result (11), integrating the momentum equation (4) from $z = 0$ to L gives

$$L\,\frac{\partial w}{\partial t} + \frac{12w}{d^2}\left(\nu_H L + \frac{\alpha\Delta T}{2L}\left(L - \frac{wd^2}{4\kappa}\right)^2\right) = \frac{p}{\rho} \quad (15)$$

Normalizing (15) and the chamber pressure equation (3) with

$$\left.\begin{array}{ll} w' = w/w_r & p' = \dfrac{pd^2}{\rho 12\nu_H L w_r} \\[2mm] Q' = Q/w_r d & y' = y/L \\[2mm] t' = t/(d^2/12\nu_H) & \end{array}\right\} \quad (16)$$

we get, after dropping the primes

$$\gamma\,\frac{\partial p}{\partial t} = Q - w + \delta\frac{\partial^2 p}{\partial y^2} \quad (17)$$

and

$$\frac{\partial w}{\partial t} + f(w) = p \quad (18)$$

The flow resistance in the slot is

$$f(w) = \begin{cases} w\left(1 + \frac{A}{2}(1 - w)^2\right) & w \leq 1 \\ w & w > 1 \end{cases} \quad (19)$$

The parameters γ and δ are given by

$$\gamma = \left(\frac{12\nu_H}{d^2}\right)^2\left(\frac{\rho L}{Ed}\right) \quad (20)$$

and

$$\delta = \left(\frac{12\overline{A}\ell_c^2}{d^3 L}\right) \quad (21)$$

The parameter γ is a measure of the ability of the chamber to expand with pressure and δ is a measure of the frictional resistance along the chamber.

3.1. One-Dimensional Flow

With no spatial dependence ($\partial/\partial y = 0$), (17) and (18) correspond to the experiments discussed in section 2. The pressure is analogous to the height of fluid in the column. The velocity w corresponds to the average velocity out of the copper tube which is directly proportional to the rate of change of the level in the column.

Equations (17), with $\partial/\partial y = 0$, and (18) can be combined to give

$$\frac{d^2w}{dt^2} + \frac{df}{dw}\frac{dw}{dt} + \frac{(w - Q)}{\gamma} = 0 \quad (22)$$

This equation has the steady fixed-point solution

$$\begin{aligned} w_0 &= Q \\ & \quad\quad\quad\quad\quad\quad\quad (23) \\ p_0 &= f(w_0) \end{aligned}$$

It is straightforward to show that this steady solution is linearly unstable when

$$\left.\frac{df}{dw}\right|_{w_0} < 0 \quad (24)$$

This inequality corresponds to a decrease in fricitional resistance (or pressure drop) with an increase in velocity. This criterion is met by equation (11) for $A > 6$ in the range given by (14) and illustrated in Figure 6.

The behavior of the nonlinear solution can be deduced by recognizing that (22) is in the form of an equation describing a mass-spring system with a nonlinear friction coefficient, here given by df/dw. The topology of df/dw is similar to the classic Van der Pol equation (for example, see Davies and James, [1966]), with a region of negative friction bounded by increasing positive friction outside of this region. For Q in the linearly unstable regime a limit cycle oscillation will always develop. When A is large and $f(w)$ has a region of large negative slope, w will oscillate between periods of nearly constant low flow and an eruptive phase in which w increases rapidly and then returns to the low flow. As A approaches the critical value of 6, the oscillations will become nearly sinusoidal. If other parameters are fixed, increasing γ causes the period of the limit cycle to increase. For Q in the stable regions the solution will asymptotically approach the steady fixed point.

This behavior is illustrated with numerical solutions to (17) and (18) with $\partial/\partial y = 0$. Figure 7a shows an example with $[A, Q, \gamma] = [50.0, 0.7, 1.0]$. We picked the parame-
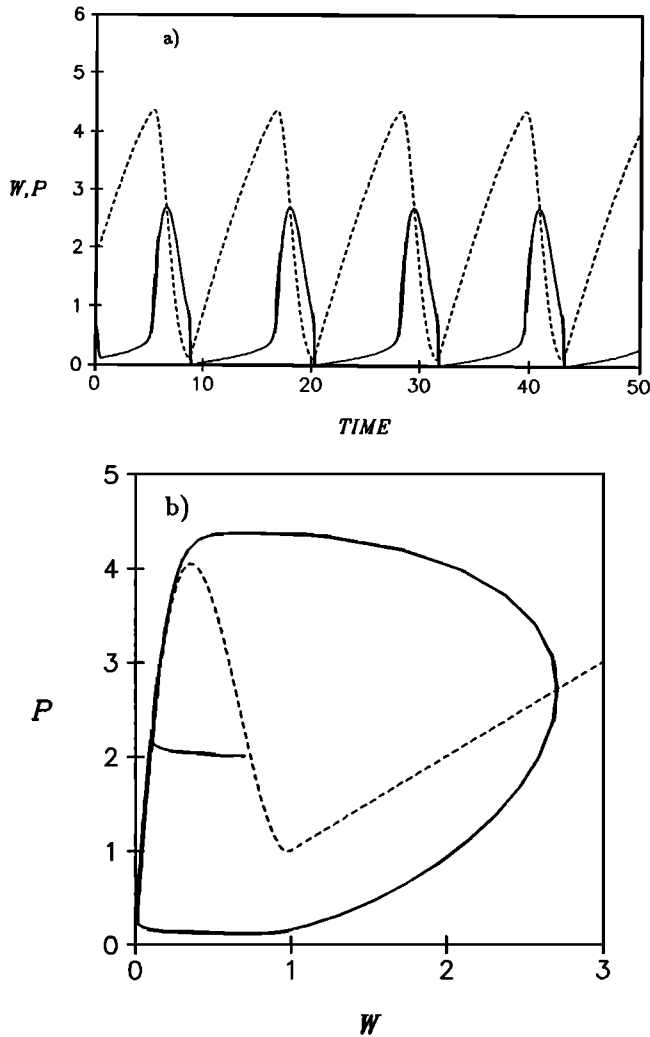
Fig. 7 (a) Numerical solution of (16) with $\partial/\partial y = 0$ and (17) for p (dashed curve) and w (solid curve) with $(A, Q, \gamma) = (50.0, 0.7, 1.0)$. (b) $p - w$ phase plane plot of the solution (solid curve). The steady state relation $p_0 = f(w)$ from (18) is also shown (dashed curve).

pressure). Increasing γ (see (20)) corresponds to a decrease in the elasticity of the chamber compared to the viscous resistance in the slot (measured by either the momentum diffusion time d^2/ν_H or the slot aspect ratio L/d). The other parameters are unchanged from Figure 7. For larger γ, the evolutions of p and w are similar to Figure 7. Increasing γ causes the period of oscillation to increase. During the deflation phase, the falloff of w is slower than for $\gamma = 1$. The $p - w$ phase plane (Figure 8b) shows that the solution approaches the high w branch of the steady solution during deflation.

One final example is shown in Figures 9a, and 9b for smaller viscosity contrast $[A, Q, \gamma] = [10.0, 0.7, 1.0]$. For this low value of A the solutions for p and w are nearly sinusoidal. The limit cycle in the $p - w$ plane forms a near ellipse around the unstable fixed point.

The behavior of the theoretical model is qualitatively similar to the experimental results shown in Figure 3. In Figures 3b and 3c the $h - v$ phase plane plots show an apparent limit cycle connecting two stable branches delineated by the results of the rundown phase of the experiment. The h versus t plot in Figure 3a shows an asymmetrical sawtooth pattern similar to p versus t in Figure 7a. Slow periods of build up of height (or pressure) are interrupted by periods of rapid
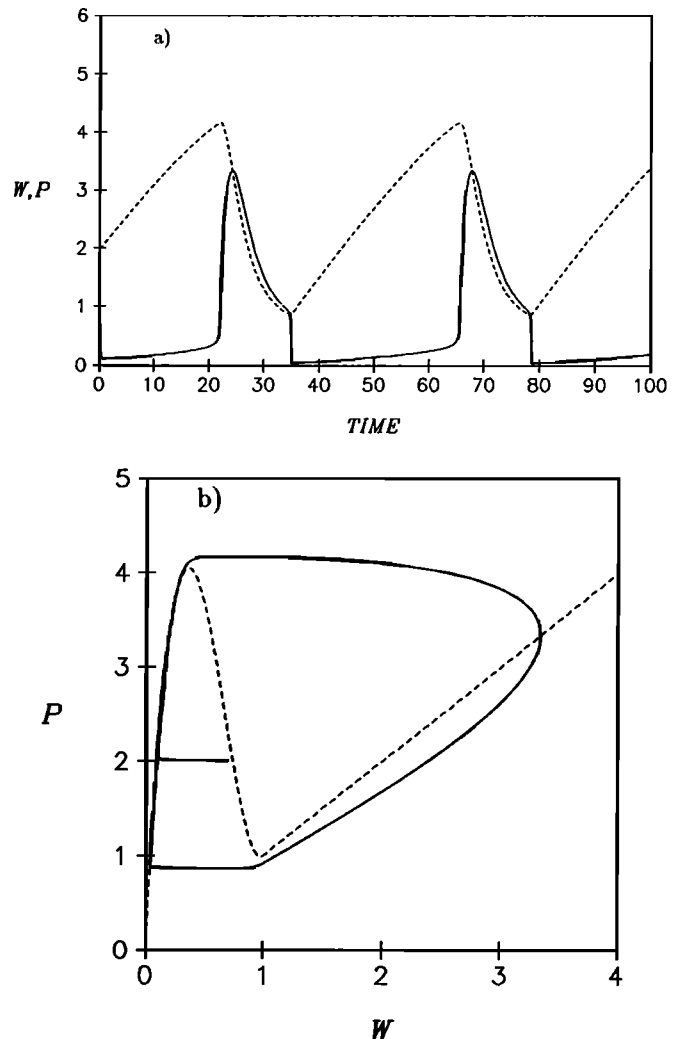
ter A large so there is a sizeable increase in viscosity. The parameter $Q = 0.7$ has been picked so the steady flow w_0 is near the center of the unstable region. The parameter γ was arbitrarily set to 1. The solution quickly achieves a limit cycle in which the flow periodically has spikes of high flow, separated by periods of low flow. The pressure p follows an asymmetrical sawtooth pattern with a slow increase during the stable low flow phase and a rapid decrease during the eruptive phase. Figure 7b shows the corresponding limit cycle in the $p - w$ phase plane. The steady relation $p_0 = f(w)$ is also plotted. The solution closely follows the stable low flow branch of the steady solution, jumping quickly across the unstable region, then looping back to the stable low flow branch. Decreasing Q increases the period of oscillation, and the eruptive phase occurs over a smaller fraction of the period. The qualitative character of the solution is unchanged from Figure 7. Increasing Q has the opposite effect. The period decreases and duration of the eruptive phase increases. Increasing (decreasing) Q causes the chamber to refill more quickly (slowly).

Figures 8a, and 8b are for a case with $\gamma = 5$ so the chamber is "weaker" (i.e., more expansive with an increase in

Fig. 8. Same as Figures 7a and 7b except $(A, Q, \gamma) = (50.0, 0.7, 5.0)$ so the chamber is more expansive.

Fig. 10. Plot of the growth rate $Re(\sigma_1)$ from (27) as a function of k^2. Here $Re(\sigma_1)$ is divided by $1/2 df/dw|_{w_0}$ and k^2 is divided by $\frac{\gamma}{\delta} df/dw|_{w_0}$. Four values of the parameter $\gamma/4 \, df/dw|_{w_0}$ are illustrated. All curves asymptote to 2 for large wavenumbers.
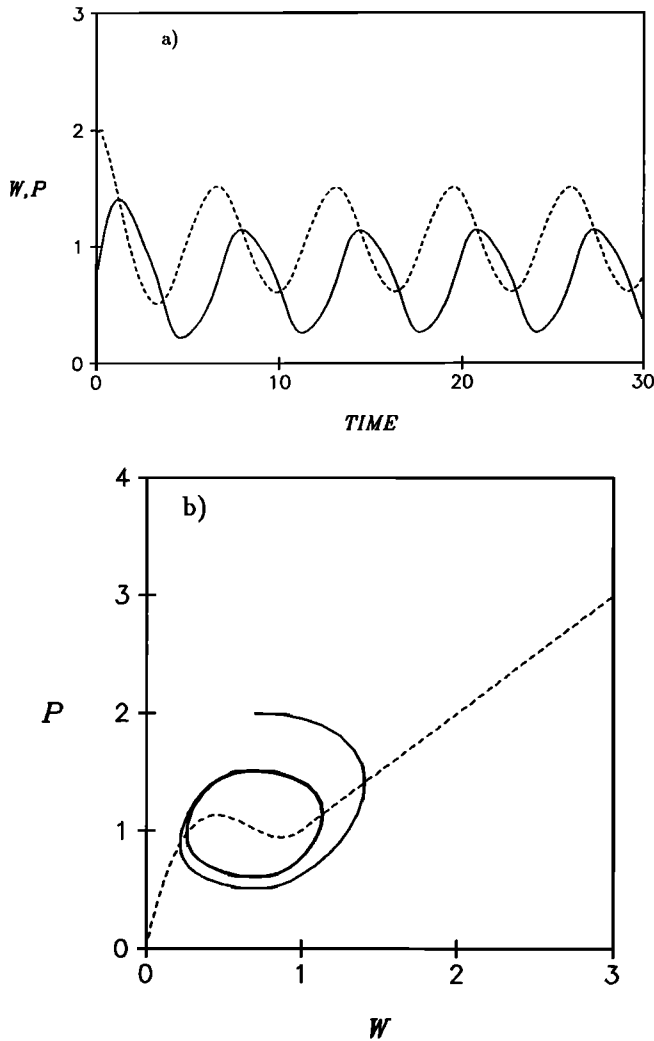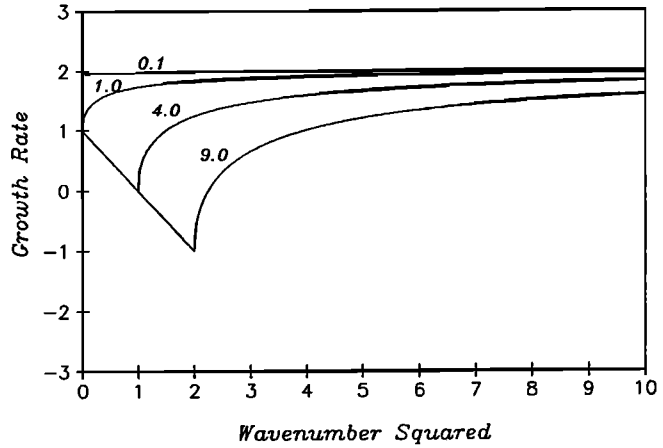

Fig. 9. Same as Figures 7a and 7b except $(A, Q, \gamma) = (10.0, 0.7, 1.0)$.

deflation and eruption. Note that when the height rapidly decreases, the temperature of the outflowing fluid rapidly rises. Finally, the plateau in the rundown experiments corresponds to a jump from the fast to the slow branch. Of course, the model is highly idealized, but it does reproduce the main features of the experiment.

3.2. Two-Dimensional Flow

We now return to the two-dimensional problem and ask whether spatial perturbations can grow. If spatial instabilities do grow the flux of fluid from an eruption would be spatially concentrated, resulting in along-slot fingering.

First, (17) and (18) are linearized about the steady solution (23) with

$$w = w_0 + \epsilon w_1$$

$$p = p_0 + \epsilon p_1 \tag{25}$$

where $\epsilon \gg 1$, and one equation for w_1 is found

$$\gamma \frac{\partial^2 w_1}{\partial t^2} + \gamma \frac{df}{dw}\bigg|_{w_0} \frac{\partial w_1}{\partial t} -$$

$$\delta \frac{\partial^3 w_1}{\partial t \partial y^2} - \delta \frac{df}{dw}\bigg|_{w_0} \frac{\partial^2 w_1}{\partial y^2} + w = 0 \tag{26}$$

Taking $w_1 = W_1 \, e^{iky+\sigma t}$, where W_1 is a constant, a quadratic dispersion relation is obtained from (26). The two roots $\sigma_{1,2}$ are given by

$$\sigma_{1,2} = -\frac{1}{2}\left[\frac{df}{dw}\bigg|_{w_0} + \frac{\delta k^2}{\gamma}\right]$$

$$\pm \left[\frac{1}{4}\left(\frac{df}{dw}\bigg|_{w_0} + \frac{\delta k^2}{\gamma}\right)^2 - \frac{1}{\gamma}\left(1 + \delta k^2 \frac{df}{dw}\bigg|_{w_0}\right)\right]^{1/2} \tag{27}$$

The real part of the plus root, σ_1, is always larger than the other root, σ_2, so we will consider σ_1 only. For $k = 0$ we recover the one-dimensional result that $df/dw|_{w_0} < 0$ is required for instability. For $k = 0$ and $\gamma \gg 1$,

$$\sigma_1 = -\frac{df}{dw}\bigg|_{w_0} + O\left(\gamma^{-1}\right) \tag{28}$$

and when $\gamma \gg 1$,

$$Re(\sigma_1) = -\frac{1}{2}\frac{df}{dw}\bigg|_{w_0} \qquad Im\,(\sigma_1) = \gamma^{-1/2} \tag{29}$$

This root is growing oscillations.

Analysis for $k \neq 0$ shows that $df/dw|_{w_0} < 0$ is still a necessary condition for instability. Since δ always multiplies k^2, it can be removed by rescaling y and therefore will be set to 1 in (27). For $k \gg 1$, (27) becomes

$$\sigma_1 = -\frac{df}{dw}\bigg|_{w_0} + O(k^{-2}) \tag{30}$$

and the root is purely real.

For $k \leq O(1)$ the behavior is slightly more complicated. Figure 10 illustrates the behavior of $Re(\sigma_1)$. For $\gamma \gg 1$, $Re(\sigma_1)$ is independent of k. As γ decreases the growth rate for $k = O(1)$ decreases until a band of wavenumbers have $Re(\sigma_1) < 0$. When $\gamma > 4/(df/dw|_{w_0})^2$ the roots are purely real. When $\gamma < 4/(df/dw|_{w_0})^2$ the roots are complex (i.e., oscillatory) for $\delta k^2 < 2\,\gamma^{-1/2} + \gamma\,(df/dw|_{w_0})$ and real for larger k^2. The transition occurs at k corresponding to the minimum of $Re(\sigma_1)$ shown in Figure 10.

The linear stability analysis of the two-dimensional problem shows that a fingering instability resulting in the lateral

concentration of outflow is possible. However, the linear analysis does not give a single wave number of maximum growth and therefore does not suggest a dominant length scale. A more complete analysis in the nonlinear regime, or an improved model incorporating lateral flow within the slot is necessary.

Before ending, it must be pointed out that the overall features of the results are not dependent upon the specific thermal model of the slot that has been adopted here. A second calculation has been made that parameterizes the temperature of fluid rising through the slot with a model equation of the form

$$w\frac{\partial T}{\partial z} = -C\,\frac{\kappa}{d^2}\,(T - T_W) \qquad (31)$$

where w is velocity through the slot and T_W is the wall temperature. The constant C is a geometrical variable that was set for convenience equal to 1. The solution is

$$T = T_W + (T_H - T_W)\,e^{-\kappa z/d^2 w} \qquad (32)$$

where T_H is temperature of the fluid in the chamber.

For this thermal model it was necessary to have viscosity dependence upon temperature be represented as a quadratic function

$$\nu = \nu_H + \alpha(T_H - T) + \beta(T_H - T)^2 \qquad (33)$$

in order to obtain a relationship between steady pressure drop p_0 and w that is anologous to (10). If β is set to zero, there is no region of decreasing pressure drop to increasing w and therefore no instability will develop.

4. Experiments With Paraffin

Experiments with liquid paraffin have been conducted that demonstrate a transition from uniform flow to fingering flow as time progresses. The apparatus consisted of a 1.2 cm thick square rolled aluminum plate 61 cm on a side placed horizontally in a pan of ice water so that the underside of the plate was in contact with the water. The temperature of the ice water is estimated to be approximately 5°C in contact with the plate, since the ice floated only around the edges of the plate. The plate was carefully placed in the water so no air was trapped under it, and then it was carefully leveled. The leveling was essential because preliminary experiments had raised the question of whether the direction of flow was influenced by poor leveling. A 1.1-cm-thick square plexiglas plate 46 cm on a side was clamped over the aluminum with spacers between the aluminum and plexiglas so a narrow gap 0.241 ± 0.007 cm remained. A hole drilled in the center of the plexiglas was connected by heated hose to a reservoir containing melted paraffin. A camera was positioned above the apparatus to take photographs every 4 s.

4.1. Qualitative Observations

As a run commenced, paraffin was delivered to the hole at a rate of 5.5 cm^3 s^{-1}. For approximately the first 16 s, the paraffin spread out in a growing pattern that was close to perfectly circular (Plate 1a). Small deviations from perfect circles appeared to be produced from surface tension effects arising from slight irregularities in the texture of the black painted aluminum, but these deviations produced less than 10% deviation in the radius of the circle. After 16 s, the cir-

cular front rapidly developed little notches (Plate 1b) that signified a sudden decrease in velocity at a point on the circle. Next to these notches, there was shortly a rapid growth of radial finger-like bulges (Plate 1c) with round tips. Ten or 12 fingers grew within 4 s but many of them stopped growing during the next 4 seconds (Plate 1d). The only change in the pattern subsequently was that four fingers reached the edge of the tank, the rest gradually froze. Oil-soluble dye was injected into the paraffin source, and it was observed that when the dye had arrived in the cell, 28 s after Plate 1d, most flux was into the two largest fingers (Plate 1e). The dye had begun to intrude into a third tube, but it apparently stopped shortly after arriving in the cell. Forty seconds later, dye of another color was injected, and by that time, flow was only going out of one finger (Plate 1f). For 40 s more, flow out through that finger continued in a clearly defined channel with little apparent change.

4.2. Quantitative Measurements

To measure the progression of the front, distances were taken from the photographs with dividers and tabulated. For the photographs with an almost circular intrusion, the extremes of the radius were measured. For the finger cases, the distance of the tip of every finger from the outside of the feeding tube was measured and one measurement was also taken in between each pair of fingers. The results are shown in Figure 11. During the time when the front was circular, the front advanced as it would from simple laws of conservation of mass; a line with the formula $r = (Qt/\pi h)^{1/2}$ is shown for comparison. In this formula the volume flux Q is 5.5 cm^3 s^{-1}, time is t and gap width h is 0.241 cm. As the fingers developed, the fronts on the fingers speeded up, and the front between fingers slowed down and finally stopped at which time the paraffin appeared to begin to solidify at the stopped regions. As time commenced, many of the smaller fronts of fingers also stopped, but the remaining ones sped up even more. The width of the final channel as marked by the colored dye varied along the channel from 1.4 to 1.7 cm.

A simple explanation of why the instability must happen is that the paraffin would become cold and very viscous if it remained in circular flow because then it would stay in the gap for more than a thermal time constant. However, it was clear that the paraffin had never completely solidified anywhere during this run; it just appears to experience a dramatic increase in bulk viscosity as it cools. Assuming that both the lid and the aluminum plate cool the paraffin as it flows along the slot, the value of the thermal time constant for the paraffin in a gap of 0.241 cm can be estimated from the formula $h^2/4k$. Using the above value of h and $k = 0.0004$ cm^2 s^{-1}, the time constant is 36 s. In the experiment the interface become unstable after 16 s. Also, the final channel of approximately 1.5 cm width admits a flow from the hole to the edge of the plate of about 15 cm/s. Therefore, fluid leaves the region after being in the slot for less than 2 seconds, a time that is short compared to the time constant estimated above. Of course, these numbers have considerable uncertainties and are meant to be only approximate, but the simple concept that a flow pattern is formed that would allow fluid to escape before it cools is consistent with the experiment.

We also estimate the parameter group $ud^2/8\kappa L$ at which the fingers were first detected. Here $u = 3Q/4\pi r d$, where $r = 13$ cm, the radius when fingering developed, and L is
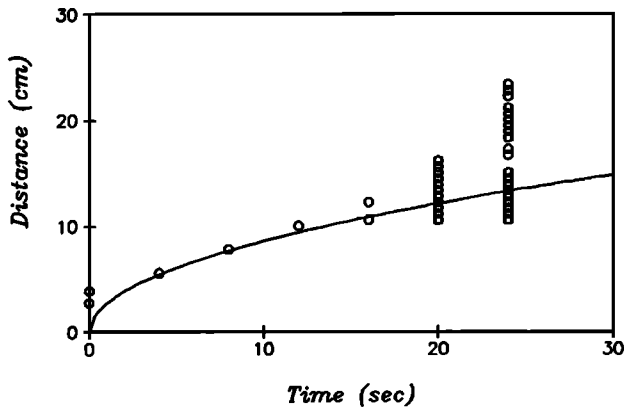
Plate 1. Photographs of the evolution of paraffin flowing with constant volume flux through a cooled slot from a point source. From left to right: (a) At 12 s after start of the experiment a circular intrusion is seen. (b) At 16 s two small notches have grown. (c) By 20 s numerous fingers break out. (d) At 24 s the fingers have grown considerably. (e) At 52 s, dye reveals there is flow through two channels; there is also evidence that third channel stopped just as the dye entered the tank. (f) At 92 s, darker dye reveals that there is flow in only one channel.

Time (sec)

Plate 1. Photographs of the evolution of paraffin flowing with constant volume flux through a cooled slot from a point source. From left to right: (a) At 12 s after start of the experiment a circular intrusion is seen. (b) At 16 s two small notches have grown. (c) By 20 s numerous fingers break out. (d) At 24 s the fingers have grown considerably. (e) At 52 s, dye reveals there is flow through two channels; there is also evidence that third channel stopped just as the dye entered the tank. (f) At 92 s, darker dye reveals that there is flow in only one channel.

also set to this radius. Using these valves and the values of Q, κ and d from above, we get

$$\frac{ud^2}{8\kappa L} = \frac{3Qd}{32\pi r^2 \kappa} = 0.6$$

This value is within the range predicted by the idealized theory (14) for $A \gg 6$, which is the case for parrifin. These are numerous differences between the experiment and the model, but the agreement is encouraging.

CONCLUDING REMARKS

The central result is that flows are unstable if Peclet number wd/κ is in the range

$$\frac{8}{3}\frac{L}{d} < \frac{wd}{\kappa} < \frac{8L}{d} \text{ for } \frac{\alpha\Delta T}{\nu_H} \gg 6$$

and

$$\frac{16}{3}\frac{L}{d} < \frac{wd}{\kappa} < \frac{8L}{d} \text{ for } \frac{\alpha\Delta T}{\nu_H} \gtrsim 6$$

Unstable flow can be either time dependent or spatially dependent. Both laboratory and numerical experiments show that time-dependent flows are periodic for the very simple one-dimesnional problem studied here. Little is known in detail about the spatially dependent system, although the linearized stability analysis indicates that fastest growth rates are for large wave numbers, or short wavelengths. The small wave numbers have growing oscillations if the chamber is expansive enough. Crude transient experiments with paraffin exhibited fingers suddenly developing as a circular front advanced over a cold plate. However, the number of advancing fingers rapidly decreased with time to one, but that one persisted for a very long time thereafter. This indicates that spatial finite amplitude behavior may be quite complicated to analyze theoretically.

A detailed application to any geological system has not yet been made, but numerous magmatic and hydrothermal systems are known to possess an increase in resistance

upon cooling. The hypothesis by *McBirney* [1984] that flow through a dyke is fundamentally unsteady and is either gradually blocked or melts away the wall, as developed by *Bruce and Huppert* [1989], seems to be the closest actual application. A study by *Lowell* [1990] attributes focusing of feeder fluid to black smokers to contraction upon cooling of the vent walls and thus is similiar in spirit to the present study, but alludes to a different mechanism. Recent gravity data [*Lin, et al.*, 1984] show that the accretion of magma at a series of segment along the Mid-Atlantic Ridge is focused at discrete centers along the spreading axis. Whether this arises from the present mechanism or from diapirism from deeper in the mantle [*Whitehead et al.*, 1984] is unknown. Finally, R. Kent (private communication 1990) has pointed out to us the presence of lamprophyre intrusions in the Damodar Valley of north east India whose cylindrical melt tubes have apparently arisen from low-viscosity melt penetrating into carbonaceous sediments. Whether these can be understood in the context of this mechanism is still open.

We close by noting there is still an enormous number of problems to be done. The finite amplitude behavior is not understood yet nor is the full two-dimensional stability problem. We wonder wheter these problems are very sensitive to geometry. Can fluid intrusions through porous flow develop similiar instabilities if the interaction between fluid and porous medium increases hydraulic resistance?

REFERENCES

Bruce, P. M., and H. E. Huppert, Thermal control of basaltic fissure eruptions, *Nature*, *342*, 665–667, 1989.

Davies, T. V., and E. M. James, *Nonlinear Differential Equations*, Addison-Wesley, 1966.

Hughes, C. J., *Igneous Petrology*, Elsevier Scientific, New York, 551 pp., 1982.

Lin, J., G. M. Purdy, H. Schouten, J. C. Sempere, and C. Zervas, Evidence from gravity data for focused magmatic accretion along the Mid-Atlantic Ridge, *Nature*, *344*, 627–632, 1990.

Lowell, R. P., Thermoelasticity and the formation of black smokers, *Geophys. Res. Lett.*, *17*, 709–712, 1990.

McBirney, A. R. *Igneous Petrology*, Freeman-Cooper, 1984. San Francisco, Calif.

Ortoleva, P., J. Chadam, E. Merino, and A. Sen, Geochemical self-organization II. The reactive-infiltration instability, *Am. J. Sci.*, *287*, 1008–1040, 1987a.

Ortoleva, P., E. Merino, C. Moore, and J. Chadam, Geochemical self-organization I: Reaction-transport feedbacks and modeling approach, *Am. J. Sci.*, *287*, 979–1007, 1987b.

Saffman, P. G. and G. I. Taylor, The penetration of a fluid into a porous medium or Hele-Shaw cell containing a more viscous liquid, *Proc. R. Soc. London Ser. A 245*, 312–329, 1958.

Whitehead, J. A., H. J. B. Dick, and H. Schouten, A mechanism for magmatic accretion under spreading centers, *Nature, 312*, 146–148, 1984.

J. A. Whitehead and K. R. Helfrich, Woods Hole Oceanographic Institution, Woods Hole, MA 02543.